

Cite this: *J. Mater. Chem.*, 2011, **21**, 11116

www.rsc.org/materials

PAPER

## Patterned fluorescence films with reversible thermal response based on the host–guest superarchitecture†

Wenyong Shi, Yanjun Lin, Shan He, Yufei Zhao, Changming Li, Min Wei,\* David G. Evans and Xue Duan

Received 24th March 2011, Accepted 3rd May 2011

DOI: 10.1039/c1jm11249j

This paper reports patterned films with thermal colorimetric and fluorescent response fabricated by a combined approach based on electrophoretic deposition (EPD)–photolithography. A composite film of diacetylene (DA)/layered double hydroxide (LDH) was prepared by the method of EPD, and the photolithography technique was subsequently employed to further obtain a polydiacetylene (PDA)/LDH patterned fluorescence film *via* UV-induced polymerization of DA in the two-dimensional (2D) gallery of LDH matrix. The PDA/LDH film shows a well *c*-orientation of LDH platelets (the *ab* plane of the LDH platelets parallel to the substrate) confirmed by XRD and SEM. Both the *in situ* UV-vis absorption and fluorescence emission spectroscopy indicate that the composite film exhibits marked thermal colorimetric and fluorescent behavior in the temperature range 20–130 °C, which is reversible over a number of heating/cooling cycles. It should be noted that the pristine PDA shows no reversible thermal colorimetric and fluorescent performance at all. The transformation of an organic chromophore from irreversible to reversible thermal response material upon incorporation into a 2D layered matrix is the most distinct feature in this work. It was demonstrated that the thermally response behavior resulted from the strong hydrogen bond interaction between the PDA and LDH matrix, which was confirmed by *in situ* Raman and *in situ* attenuated total reflection Fourier-transform infrared (ATR FT-IR) spectroscopy. Therefore, this work provides new opportunities for the fabrication of thermally responsive patterned films with high stability and reversibility, which can be used in intelligent response and display devices.

### 1. Introduction

Conjugated polydiacetylenes (PDAs) derived from the polymerization of 1,3-diacetylene (DA) derivatives have attracted great attention during the past few years, owing to their functionalizability and applicability in colorimetric detection systems.<sup>1</sup> Unique “blue-to-red” colorimetric transition of variously modified PDA derivatives has been utilized to monitor ligand–receptor binding events involving viruses,<sup>2</sup> toxins,<sup>3</sup> glucose<sup>4</sup> and ionic interactions.<sup>5</sup> Solution-phase sensing was normally disadvantageous in terms of signal intensity and/or applicability to miniaturized sensor systems, which greatly limited the wide application of PDAs. To solve these problems, many efforts have been made by immobilization of PDAs onto

glass, quartz, silicon and polystyrene substrates;<sup>6</sup> however, the resultant materials generally suffer from poor stability, processability, response time and sensitivity. Therefore, it is highly essential to search for novel materials to immobilize the PDAs for achieving sensor and array devices with high stability, reusability and environmental compatibility.

In recent years, considerable interest has been focused on the fabrication of conjugated polymer–inorganic composite materials, since they may show novel functionalities (ascendant photo-, thermal- and mechanical-stabilization), which are not present in the individual components alone. Layered double hydroxides (LDHs), whose structure can be generally expressed as  $[M^{II}_{1-x}M^{III}_x(OH)_2](A^{n-})_{x/n} \cdot mH_2O$  ( $M^{II}$  and  $M^{III}$  are divalent and trivalent metals respectively;  $A^{n-}$  an  $n$ -valent anion), are one type of important layered materials which represent a large versatility in terms of chemical composition and capability to build up 2D-organized structures (stacking of the host layers gives rise to an accessible interlayer space in the nanometre scale).<sup>7</sup> The incorporation of polymer monomer into the LDH gallery for *in situ* preparation of polymer–LDH composites exhibits the following advantages: firstly, LDH provides a confined reaction region for controlling the monomer polymerization (molecular weight, products distribution); secondly,

State Key Laboratory of Chemical Resource Engineering, Beijing University of Chemical Technology, Beijing, 100029, China. E-mail: weimin@mail.buct.edu.cn; Fax: +86-10-64425385; Tel: +86-10-64412131

† Electronic Supplementary Information (ESI) available: The optical microscopic images (Fig. S1); The patterned film of the physical mixture sample (Fig. S2); the UV-vis absorption spectra (Fig. S3); the *in situ* UV-vis spectra of the physical mixture sample (Fig. S4); the TG-DTA curves (Fig. S5); the storage stability measurements (Fig. S6); AFM images (Fig. S7); the *in situ* Raman spectra (Fig. S8) and the *in situ* ATR FT-IR spectra (Fig. S9).

the intrinsically anisotropy of the LDH matrix imparts a high orientation and configuration to the polymers, which are expected to exhibit advanced physicochemical properties; thirdly, the presence of the LDH matrix would improve the stability (optical, thermal and mechanical) and environmental compatibility of the functional polymer molecules.

Recently, patterning the chemical properties of films has attracted great attention in the field of miniaturized sensor design and molecular electronics.<sup>8</sup> Patterned films can control the localized interfacial properties including electron conduction pathways and the spatially interfacial gradient required for interfacially driven fluid and particle flow. Many patterning techniques have been reported, including selective deposition,<sup>9</sup> polymer-on-polymer stamping,<sup>10</sup> capillary transfer lithography,<sup>11</sup> imprinting,<sup>12</sup> spin coating<sup>13</sup> and microfluidic patterning.<sup>14</sup> The photolithography method, achieved by using a mask or aperture to localize the photochemistry spatially, is an efficient tool for microfabrication in a broad range of applications in science and technology.<sup>15</sup> This technique has gained increasing interest due to its versatility, flexibility and rapid processability. This gives us impetus to challenge the goal of fabricating patterned films by the photolithography method, for the purpose of obtaining array sensors and devices with high stability and reusability.

The PDA-based chemosensors reported to date generally function in a irreversible fashion, because the blue-phase shifts to the red-phase upon a given external stimulus while the backward "red-to-blue" transition does not occur even though the stimulus is removed from the system. Therefore, how to improve their reversible luminescence response remains a challenge. In this work, DA molecule intercalated LDH composite films were fabricated by the electrophoretic deposition (EPD) method, and the photolithography technique was employed to further obtain patterned films which show thermal colorimetric and fluorescent response with high stability and reversibility. Furthermore, the film with a thickness of 500 nm exhibits thermal colorimetric and fluorescent behavior with fast response due to the strong hydrogen bond interactions between host and the guest, which was confirmed by *in situ* Raman and *in situ* attenuated total reflection Fourier-transform infrared (ATR FT-IR) spectroscopy. It is expected that the strategy reported here can be employed to fabricate a variety of patterned images with interesting thermally-driven behavior, which can be used in the fields of intelligent response and display.

## 2. Experimental section

### 2.1 Materials

Diacetylene (DA, biochemistry grade) was purchased from Sigma-Aldrich. Analytical grade chemicals including  $\text{Mg}(\text{NO}_3)_2 \cdot 6\text{H}_2\text{O}$ ,  $\text{Al}(\text{NO}_3)_3 \cdot 9\text{H}_2\text{O}$ , NaOH, tetrahydrofuran (THF) and  $\text{C}_2\text{H}_5\text{OH}$  were used without further purification. Deionized and decarbonated water was used in all the experimental processes.

### 2.2 Synthesis of the DA-LDH colloid suspension

The  $\text{Mg}_2\text{Al-NO}_3$  LDH precursor was synthesized by the hydrothermal method.<sup>16</sup> Subsequently, the DA intercalated

LDH colloid composite was prepared following the ion-exchange method. DA ( $10^{-3}$  mol) was dissolved in 150 mL of water-THF mixture solvent (1 : 1, v/v). Freshly prepared  $\text{Mg}_2\text{Al-NO}_3$  LDH colloid (40 mL,  $0.025 \text{ g mL}^{-1}$ ) was dispersed in the mixture solution thoroughly. The suspension was agitated at room temperature under  $\text{N}_2$  atmosphere for 48 h. The DA-LDH colloidal suspension was obtained by washing extensively with water and then dispersing in ethanol ( $0.01 \text{ g mL}^{-1}$ ).

### 2.3 Fabrications of the DA-LDH thin film

ITO Substrates were firstly cleaned by immersing in a bath of deionized water and ethanol (1 : 1, v/v) in an ultrasonic bath for 30 min. The DA-LDH thin film was fabricated by the EPD method. Ethanol was used as a dispersion medium to prepare the colloidal nanoparticle suspension of DA-LDH ( $0.005 \text{ g mL}^{-1}$ ). Two ITO substrates were used as the working and counter electrode respectively, which were placed parallel with a distance of 1 cm. The voltage between the two electrodes was set at 10 V and the electrophoretic time was 5 min.

### 2.4 Fabrication of the patterned PDA-LDH thin film

The patterned PDA-LDH thin film was obtained by irradiating the DA-LDH thin films with 254 nm UV light for 5 min through a photomask with 50 and 500  $\mu\text{m}$  wide line, respectively. This process induced photopolymerization of DA in the LDH gallery in the exposed areas.

### 2.5 Characterization techniques

The powder XRD measurements were performed on a Rigaku XRD-6000 diffractometer, using  $\text{Cu K}\alpha$  radiation ( $\lambda = 0.15418 \text{ nm}$ ) at 40 kV, 30 mA, with a scanning rate of  $5^\circ \text{ min}^{-1}$ , and a  $2\theta$  angle ranging from  $2^\circ$  to  $65^\circ$ . SEM images were obtained using a ZEISS scanning electron microscope. The UV-vis spectra were collected on a Shimadzu U-3000 spectrophotometer. Fluorescence emission spectra were recorded on a RF-5301PC fluorophotometer (1.5 nm resolution) in the range 500–650 nm with the excitation wavelength of 490 nm and slit width of 3 nm. The attenuated total reflection Fourier-transform infrared (ATR FT-IR) spectra were recorded using a Vector 22 (Bruker) spectrophotometer in the range  $4000\text{--}400 \text{ cm}^{-1}$  with  $4 \text{ cm}^{-1}$  of resolution. Elemental analysis samples were prepared by dissolving 30 mg of solid sample with a few drops of concentrated  $\text{HNO}_3$  and diluted to 50 mL with water. Mg and Al elemental analysis was performed by atomic emission spectroscopy with a Shimadzu ICPS-7500 instrument. C, H, N content was determined using an Elementar vario elemental analysis instrument. The water content of the sample was obtained by thermogravimetry. Fluorescence images were observed using an OLYMPUS-BX51 fluorescence microscope. Steady-state polarized photoluminescence measurements were recorded with an Edinburgh Instruments' FLS 920 fluorimeter. The surface roughness and thickness data were obtained by using the atomic force microscopy (AFM) software (Digital Instruments, version 6.12). The Raman spectra were obtained with 514.5 nm of excitation by using a confocal Raman microspectrometer (Renishaw Instruments Co. Ltd., RM2000) in the range

800–2200  $\text{cm}^{-1}$ . The heating/cooling speed is  $10^\circ \text{min}^{-1}$  in all the *in situ* measurements.

### 3. Results and discussion

#### 3.1 Structural and morphological characterization

The XRD patterns of the  $\text{Mg}_2\text{Al-NO}_3$  LDH precursor and the resulting PDA-LDH powder and thin film samples are shown in Fig. 1. All the patterns of these samples can be indexed to a hexagonal lattice. The interlayer spacing can be calculated from averaging the positions of the three harmonics:  $c = 1/3 (d_{003} + 2d_{006} + 3d_{009})$ . The (003) reflection of  $\text{Mg}_2\text{Al-NO}_3$  LDH powder sample at  $2\theta = 9.9^\circ$  (Fig. 1A curve a) shows an interlayer distance of 0.88 nm. The basal spacing of the PDA-LDH composite (Fig. 1A curve b) increased to 2.01 nm as a result of intercalation of DA and its resulting polymerization reaction. Compared with the PDA-LDH powder sample (Fig. 1A curve b), the PDA-LDH thin film (Fig. 1A curve c) displays only one series of  $00l$  reflections, indicating a highly ordered stacking of the *ab* plane of LDH platelets parallel to the substrate. The SEM image of the PDA-LDH thin film exhibits a smooth and continuous surface in the top view (Fig. 1B). High magnification of the film (Fig. 1C) demonstrates that the PDA-LDH nanoplatelets (100~200 nm) are densely packed on the substrate plane with well *c*-orientation, consistent with the XRD results. The side-view of SEM image shows a thickness of 500 nm for the PDA-LDH film on a quartz substrate (Fig. 1D). The chemical composition of the PDA-LDH composite was found to be  $[\text{Mg}_{0.67}\text{Al}_{0.33}(\text{OH})_2] (\text{DA})_{0.31}(\text{OH})_{0.02} \cdot 1.12\text{H}_2\text{O}$  based on the elemental analysis and TG-DTA results.

#### 3.2 Patterning of the PDA-LDH thin film and its thermal response behavior

In order to achieve the patterned PDA-LDH thin film with thermochromic and fluorescent behavior, a photolithographic method was employed (Fig. 2). Firstly, the DA-LDH thin film

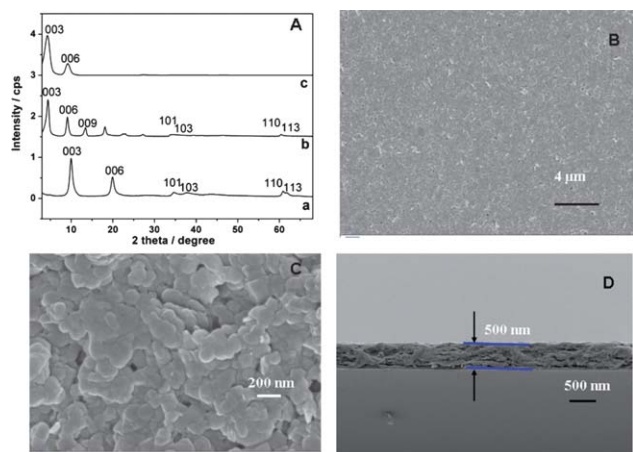


**Fig. 1** (A) XRD patterns for (a)  $\text{Mg}_2\text{Al-NO}_3$  LDH powder sample, (b) PDA-LDH powder sample and (c) PDA-LDH film; top-view of SEM images for the PDA-LDH film at (B) low magnification and (C) high magnification; (D) side-view of SEM image for the PDA-LDH film on a quartz substrate.

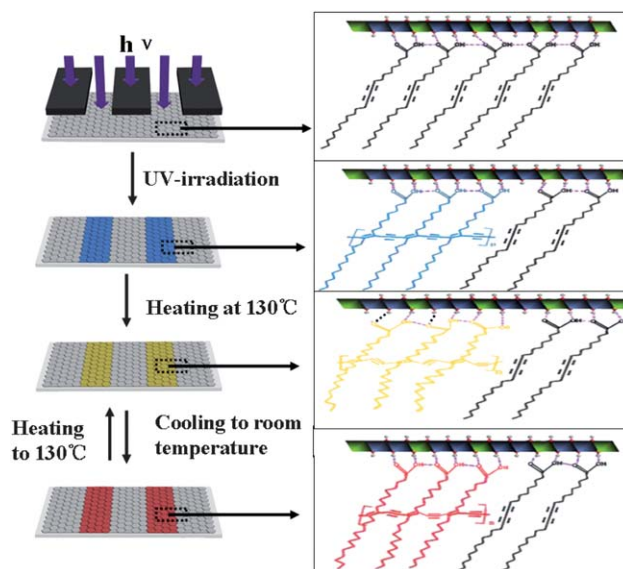


**Fig. 2** Schematic representation for the generation of patterned images of the PDA-LDH thin film.

was irradiated with 254 nm UV light for 5 min through a photomask, which induced photopolymerization of DA in the LDH gallery in the exposed areas to produce the blue phase. Then, the film was heated at 130  $^\circ\text{C}$  for 1 min to cause the blue-to-yellow color change of the PDA molecule. Finally, the film is cooled down to room temperature leading to the formation of the red phase. Upon repeating such thermal cycle between room temperature and 130  $^\circ\text{C}$ , the reversible color change between red and yellow can be observed.

Fig. 3 shows optical (top) and fluorescence microscopic (below) images of the PDA-LDH thin film induced by photomasked irradiation with two different wide line (500 and 50  $\mu\text{m}$ ). UV irradiation of the colorless DA-LDH film results in the formation of patterned blue/colorless image with 500  $\mu\text{m}$  wide line, confirming a successful photoinduced polymerization of the interlayer DA monomer in the UV-exposed areas (Fig. 3B, top). Heating the film at 130  $^\circ\text{C}$  causes the transition to yellow/colorless patterned image (Fig. 3C, top); while it

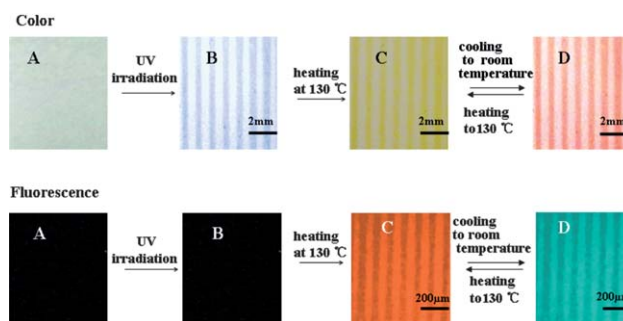


**Fig. 3** Patterned film of PDA-LDH induced by UV irradiation and its thermochromic behavior (top: 500  $\mu\text{m}$  wide line) and fluorescent transition (below: 50  $\mu\text{m}$  wide line): (A) the DA-LDH film, (B) the patterned PDA-LDH film obtained by UV irradiating (A) for 5 min, (C) the patterned film by heating (B) at 130  $^\circ\text{C}$  for 1 min, (D) the patterned film by cooling (C) to room temperature.

transfers to red/colorless patterned image as the film is cooled down to room temperature (Fig. 3D, top). In the case of the photoemission behavior, no fluorescence image was found for both the DA-LDH film and the resulting PDA-LDH film *via* UV light irradiation, since DA and blue phase PDA is non-fluorescent (Fig. 3A and 3B, below). The heat-treatment at 130 °C shows an orange-yellow/colorless patterned fluorescence image with 50  $\mu\text{m}$  wide line (Fig. 3C, below), which displays a bluish-green/colorless patterned fluorescence image when the sample is cooled to room temperature (Fig. 3D, below). Upon repeating such thermal cycle between 20 and 130 °C, the reversible color and fluorescence images of the PDA-LDH thin film can be obtained. In addition, a patterned film of PDA-LDH with 500  $\mu\text{m}$  square and 500  $\mu\text{m}$  spacing was fabricated *via* a similar method, which shows the same chromatic reversibility with the line-type patterned film (as shown in Fig S1†). In contrast, for the corresponding patterned film prepared with physical mixture of PDA and LDH, no significant thermal response for the optical and fluorescence image was observed in the temperature range 20–130 °C (Fig. S2†). Therefore, it can be speculated the thermal response performance is relevant to the host-guest interaction, which will be further discussed in the next section.

### 3.3 Thermal response reversibility of the PDA-LDH thin film

For the colorless DA-LDH thin film, no absorption band was found (Fig. S3† curve a). After UV-irradiation, a sharp absorption band at 627 nm (excitonic band) and a vibronic shoulder at  $\sim 590$  nm due to  $\pi$ -conjugated poly (ene-yne)s structure appeared,<sup>17</sup> indicating the formation of PDA with high conjugation length in the LDH gallery (blue phase, Fig. S3† curve b). Upon heating at 130 °C, a single broad peak at 494 nm attributed to  $\pi$ - $\pi^*$  electronic transition of the yellow PDA phase was observed (Fig. S3† curve c), suggesting the conformational degradation of the polymethylene chain in PDA and/or the decrease in its order degree.<sup>18</sup> After cooling to 20 °C, the PDA-LDH thin film showed absorption bands consisting of a sharp one at 530 nm (electronic band) and a broad one at 494 nm (vibronic band) (red phase, Fig. S3† curve d).

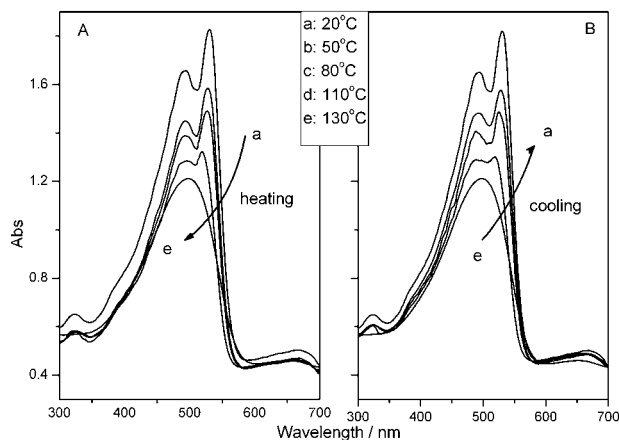


**Fig. 4** The *in situ* UV-vis absorption spectra of the PDA-LDH thin film in a (A) heating and (B) cooling cycle in the temperature range 20–130 °C.

In order to monitor the spectral change in a heating/cooling cycle, *in situ* UV-vis absorption spectra of the PDA-LDH thin film were recorded (Fig. 4). As the temperature increased from 20 to 130 °C, the intensity of the two absorption bands decreased gradually; the band at 530 nm (red phase) disappeared and only a single broad band at  $\sim 494$  nm (yellow phase) was observed at 130 °C (Fig. 4A). As the film was cooled to 20 °C, it showed converse spectral changes with the entirely recovered two bands at 494 and 530 nm (Fig. 4B). In contrast, the physical mixture sample film (PDA and LDH) showed increasing absorption at 490 and 530 nm without shift during heating from 20 to 80 °C; then the absorption intensity decreased upon further increasing the temperature to 130 °C (Fig. S4†). The absorption spectrum did not recover to its original form after cooling back to 20 °C. The contrastive results indicate that the degree conjugation of the  $\pi$  electrons along the polymer backbone changes reversibly between the red phase (530 nm) and the yellow phase (494 nm) for the PDA-LDH thin film in the temperature range 20–130 °C.

The fluorescence properties of PDA exhibit very important and attractive features. In order to study the fluorescence reversibility of the PDA-LDH thin film, the emission spectra were measured and displayed in Fig. 5. During heating the PDA-LDH thin film from 20 to 130 °C, the emission band moves from 591 to 615 nm with a concomitant gradual decrease in the luminescence intensity. The red shift and the intensity decrease of the emission peak may be attributed to the reduction of PDA order (the side chains and the backbones) and/or the enhancement of nonradiative decay processes caused by molecular thermal fluctuations. As the film is cooled to room temperature, it recovers its original emission wavelength and intensity completely accompanying with converse spectral change (Fig. 5B). The reversible fluorescence performance can be readily repeated in 20 consecutive cycles with a relative standard deviation (RSD) of 0.61% (20 °C) and 3.26% (130 °C) (Fig. 5C). In addition, TG-DTA analysis (Fig. S5†) showed that the exothermic peak of the PDA-LDH thin film occurs at  $\sim 327$  °C, higher than that of the pure PDA by  $\sim 40$  °C, indicating the thermal stability of PDA is enhanced in the LDH gallery. The storage stability test (at 20 and 130 °C, respectively) of the

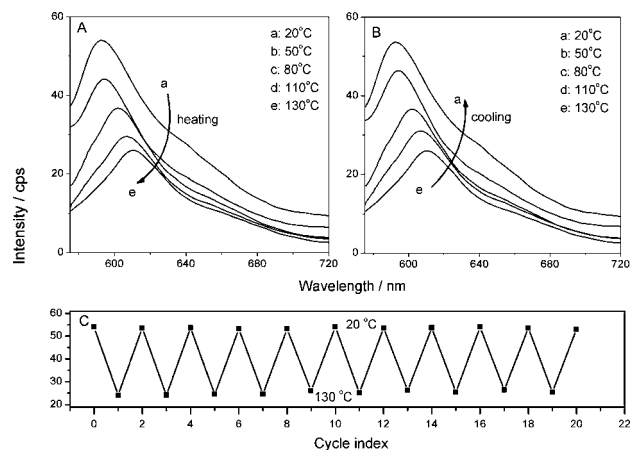


**Fig. 5** The *in situ* fluorescence spectra of the PDA-LDH thin film in a (A) heating and (B) cooling cycle in the temperature range 20–130 °C; (C) The fluorescence responses over 10 consecutive cycles.

PDA-LDH thin film shows that  $\sim 93\%$  of its initial fluorescence intensity remains after one month of measurement (Fig. S6†). Therefore, the PDA-LDH thin film possesses good reversibility and stability due to the confinement effect of LDH matrix on the intercalated PDA species, which can serve as a promising material for future practical applications.

### 3.4 The mechanism of thermal response reversibility

It was reported that the pristine PDA sample does not show reversible colorimetric and fluorescent against temperature.<sup>19</sup> In order to give a further insight for the mechanism of reversibility of the PDA-LDH thin film in this work, the polarized photoemission spectra were measured and displayed in Fig. 6. One common method to evaluate fluorescence polarization is the measurement of anisotropic value  $r$ , which reveals the average angular displacement depending upon the rate and extent of rotational diffusion for fluorophore during the lifetime of the excited state. The rate of rotational diffusion relates to the micro-environment (solvent viscosity, polarity, temperature etc.), the structure, shape and orientation of the rotating molecule.<sup>20</sup> At 20 °C, the PDA-LDH thin film shows well-defined fluorescence anisotropy between the parallel and perpendicular to excitation polarized direction with an  $r$  value of 0.31 due to the ordered arrangement of PDA in the LDH gallery (Fig. 6A). However, the value of  $r$  decreases to 0.20 at 130 °C (Fig. 6B). This indicates that the ordering degree of PDA decreases at higher temperature, associated with the increase in molecular mobility. After being cooled to 20 °C, the fluorescence anisotropy value increases to 0.30 again (Fig. 6C). The reversible change in anisotropy can also be recycled and the RSD of 10 cycles was 1.34% (20 °C) and 2.56% (130 °C), indicating that the thermal stimulus induces regular changes in ordering/orientation of PDA. Based on the fundamental rule of anisotropy and experimental results, it is proposed that the change in the  $r$  of PDA-LDH patterned film is indicative of the successive change in the orientation (polarization) of the PDA molecules in the LDH gallery in the temperature range 20–130 °C. In addition, Fig. S7† shows AFM images of the PDA-LDH thin film during a complete heating/cooling

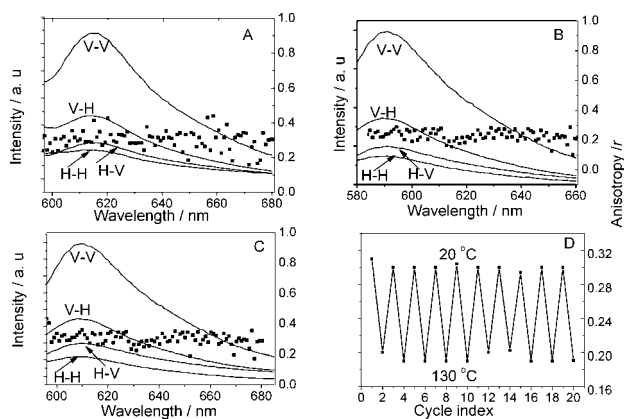


**Fig. 6** Photoemission profiles of the PDA-LDH thin film and anisotropy of the sample (scatter diagram): (A) at 20 °C, (B) heating (A) to 130 °C, (C) cooling (B) to 20 °C and (D) the fluorescence anisotropy over 10 cycles. The excitation wavelength is 530 nm.

process. At 20 °C, the PDA-LDH thin film surface was smooth with a large number of round protuberances and a root-mean square roughness of 14.9 nm (Fig. S7A†); while sharp peaks were observed after heating at 130 °C accompanied with a marked increase in RMS roughness (22.7 nm) (Fig. S7B†). After cooling to 20 °C, a relatively smooth surface was recovered with a RMS roughness of 15.8 nm (Fig. S7C†). These temperature-dependent properties (anisotropic value, surface roughness) can be ascribed to the changes in the molecular ordering/orientation of PDA in the LDH gallery.

The conformational change in the ene-yne backbone and methylene side-chain of PDA from planar to nonplanar is of major importance, since it leads to the colorimetric and fluorescent transition.<sup>21</sup> Fig. 7 displays the *in situ* Raman spectra in the temperature range 20–130 °C. For both C≡C and C=C bonds, the Raman absorption positions remain unchanged at 2114 and 1509 cm<sup>-1</sup>, respectively as the temperature increases from 20 to 130 °C, indicating no change in average conjugation length of the  $\pi$  electrons of PDA.<sup>22</sup> The gradual decrease in intensity is caused by the increase in intermolecular mobility (collisions, vibrations and rotations, etc.) for the PDA molecule (Fig. 7A). During cooling back to 20 °C, the bands of C≡C and C=C recover to their original intensity (Fig. 7B). In contrast, the physical mixture sample (PDA and LDH) reveals irreversible Raman shifts from 2116 to 2149 cm<sup>-1</sup> (C≡C) and from 1511 to 1563 cm<sup>-1</sup> (C=C) as well as a continuous decrease in intensity in a whole cycle between 20 and 130 °C (Fig. S8†), suggesting a considerable and irreversible collapse of the PDA conjugation.

To further study the effect of host-guest interaction on the conformational change in side-chain of PDA, the ATR FT-IR spectroscopic analyses were executed for the pristine PDA film, LDH film and PDA-LDH film (Fig. 8A). The pure PDA film shows methylene stretching band ( $\nu_a(\text{CH}_2) = 3016$  and  $\nu_s(\text{CH}_2) = 2952$  cm<sup>-1</sup>) and a carbonyl stretching band ( $\nu(\text{C}=\text{O}) = 1690$  cm<sup>-1</sup>);<sup>23</sup> the LDH film displays hydroxyl band ( $\nu(\text{OH}) = 3390$  and 1650 cm<sup>-1</sup>). In the case of the PDA-LDH thin film, all these five bands were observed, indicating the intercalation of PDA into the LDH gallery. *In situ* ATR FTIR analyses revealed detailed information for the PDA-LDH film upon thermal stimulus (Fig. 8B). Both the  $\nu_a(\text{CH}_2)$  and  $\nu_s(\text{CH}_2)$

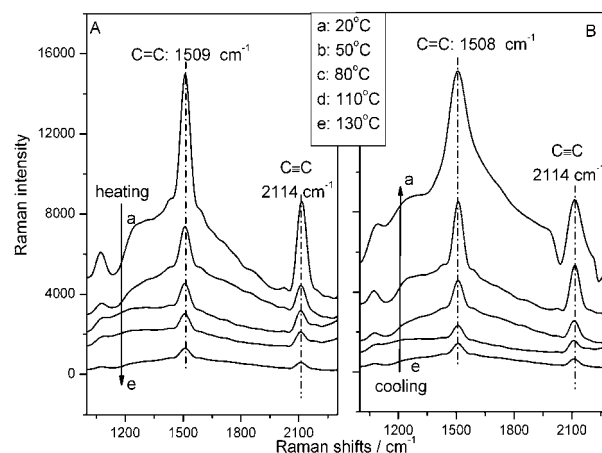


**Fig. 7** The *in situ* Raman spectra of the PDA-LDH thin film during a whole heating/cooling cycle between 20 and 130 °C.

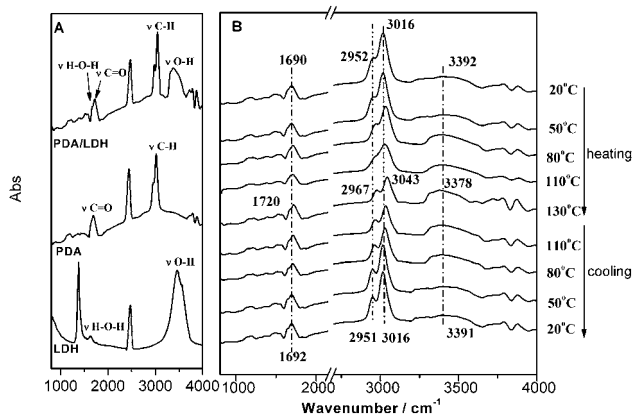


**Fig. 8** (A) ATR FT-IR spectra of pristine PDA film, the LDH film and the PDA-LDH film; (B) the *in situ* ATR FT-IR spectra of the PDA-LDH thin film in a whole heating/cooling cycle.

of the PDA-LDH film shift to higher frequency (from 3016 to 3043  $\text{cm}^{-1}$  and from 2952 to 2967  $\text{cm}^{-1}$ , respectively) with the decrease in band intensity as the temperature is raised to 130  $^{\circ}\text{C}$ , indicating that the transition dipole moment of  $\nu(\text{CH}_2)$  becomes unparallel to the conjugate plane of backbone due to re-orientation of the pendant alkyl side chains towards the conjugate plane. The  $\nu(\text{C}=\text{O})$  and  $\nu(\text{O}-\text{H})$  shift to high (from 1690 to 1720  $\text{cm}^{-1}$ ) and low frequency (from 3392 to 3378  $\text{cm}^{-1}$ ) respectively, and their intensity shows no significant change as the temperature increases from 20 to 130  $^{\circ}\text{C}$ . This indicates the formation of strong hydrogen bonds between the PDA ( $\text{C}=\text{O}$ ) and LDH layer ( $\text{O}-\text{H}$ ). In the cooling process to room temperature, converse spectral changes were observed for  $\nu(\text{CH}_2)$ ,  $\nu(\text{C}=\text{O})$  and  $\nu(\text{O}-\text{H})$ . For the comparison sample of pure PDA film however, the  $\nu(\text{C}=\text{O})$  shows an irreversible shift (from 1690 to 1708  $\text{cm}^{-1}$ ) and continuous intensity decrease in a whole temperature cycle between 20 and 130  $^{\circ}\text{C}$  (Fig. S9†). Based on the results above, it can be concluded that the hydrogen bonds between PDA and the LDH matrix plays a key role in the reversible thermal response of the guest. The transformation of an organic chromophore from a irreversible to a reversible thermal response material upon incorporation into a 2D layered matrix is the most distinct feature in this work.

#### 4. Conclusions

The highly oriented DA-LDH thin film on ITO substrates was obtained *via* the EPD method; the patterned PDA-LDH thin film was subsequently prepared through the photolithography method by UV irradiation of the DA-LDH thin film with a photomask. The patterned PDA-LDH thin film showed significant and reversible thermal colorimetric and fluorescent performance in the temperature range 20–130  $^{\circ}\text{C}$ . These temperature-dependent properties (UV absorption, fluorescence emission, anisotropic value, surface roughness) can be ascribed to the changes in the molecular ordering/orientation of PDA in the LDH gallery. In addition, the thin film possesses high stability and good reversibility owing to the formation of strong hydrogen bonds between PDA ( $\text{C}=\text{O}$ ) and the LDH layer ( $\text{O}-\text{H}$ ), which was confirmed by the ATR FT-IR spectra.

Therefore, this work provides a facile and efficient methodology for the fabrication of patterned films with attractive thermal colorimetric and fluorescent behavior. Combining the patterning technique with the thermal responsive photoluminescence nature of the chromophore-LDH composites can be widely applicable to the development of intelligent devices and display systems.

#### Acknowledgements

This project was supported by the 973 Program (Grant No.: 2011CBA00504), the National Natural Science Foundation of China, the 111 Project (Grant No.: B07004), the Postdoctoral Science Foundation (Grant No.: 20100480183) and the Collaboration Project from the Beijing Education Committee.

#### References

- (a) S. M. Ryu, I. S. Yoo, S. Song, B. Yoon and J. M. Kim, *J. Am. Chem. Soc.*, 2009, **131**, 3800; (b) J. Yoon, S. K. Chae and J. M. Kim, *J. Am. Chem. Soc.*, 2007, **129**, 3038; (c) A. Sarkar, S. Okada, H. Matsuzawa, H. Matsuda and H. Nakanishi, *J. Mater. Chem.*, 2000, **10**, 819; (d) H. J. Cho, K. Seo, C. J. Lee, H. Yun and J. Y. Chang, *J. Mater. Chem.*, 2003, **13**, 986.
- (a) A. Pevzner, S. Kolusheva, Z. Orynbayeva and R. Jelinek, *Adv. Funct. Mater.*, 2008, **18**, 242; (b) D. H. Charych, J. O. Nagy, W. Spevak and M. D. Bednarski, *Science*, 1993, **261**, 585; (c) A. Reichert, J. O. Nagy, W. Spevak and D. H. Charych, *J. Am. Chem. Soc.*, 1995, **117**, 829.
- (a) G. Y. Ma and Q. Cheng, *Langmuir*, 2005, **21**, 6123; (b) H. Zuilhof, H. M. Barentsen, M. van Dijk, E. J. R. Sudhölter, R. J. O. M. Hoofman, L. D. A. Siebbeles, M. P. de Haas, J. M. Warman, *Supramolecular Photosensitive and Electroactive Materials*; H. S. Nalwa, Ed.; Academic Press: New York, 2001, p 339, and the references cited therein.
- Q. Cheng and R. C. Stevens, *Adv. Mater.*, 1997, **9**, 481.
- (a) S. Kolusheva, T. Shahal and R. Jelinek, *J. Am. Chem. Soc.*, 2000, **122**, 776; (b) Y. K. Jung, T. W. Kim, J. Kim, J. M. Kim and H. G. Park, *Adv. Funct. Mater.*, 2008, **18**, 701.
- (a) R. Jelinek and S. Kolusheva, *Biotechnol. Adv.*, 2001, **19**, 109; (b) R. Jelinek, *Drug Dev. Res.*, 2000, **50**, 497; (c) A. Sarkar, S. Okada, H. Matsuzawa, H. Matsuda and H. Nakanishi, *J. Mater. Chem.*, 2000, **10**, 819; (d) S. Okada, S. Peng, W. Spevak and D. H. Charych, *Acc. Chem. Res.*, 1998, **31**, 229.
- (a) G. R. Williams and D. O'Hare, *J. Mater. Chem.*, 2006, **16**, 3065; (b) A. Ragavan, G. R. Williams and D. O'Hare, *J. Mater. Chem.*, 2009, **19**, 4211; (c) F. Millange, R. I. Walton, L. Lei and D. O'Hare, *Chem. Mater.*, 2000, **12**, 1990; (d) A. M. Fogg, G. R. Williams, R. Chester and D. O'Hare, *J. Mater. Chem.*, 2004, **14**, 2369.
- (a) N. Goubet, Y. Ding, M. Brust, Z. L. Wang and M. P. Pileni, *ACS Nano*, 2009, **3**, 3622; (b) S. Xu, Y. Wei, M. Kirkham, J. Liu, W. J. Mai, D. Davidovic, R. L. Snyder and Z. L. Wang, *J. Am. Chem. Soc.*, 2008, **130**, 14958; (c) C. T. Huang, J. H. Song, W. F. Lee, Y. Ding, Z. Y. Gao, Y. Hao, L. J. Chen and Z. L. Wang, *J. Am. Chem. Soc.*, 2010, **132**, 4766; (d) Y. H. Zhang, D. Zhao, X. X. Tan, T. B. Cao and X. Zhang, *Langmuir*, 2010, **26**, 11958; (e) S. Inagi, Y. Ishiguro, M. Atobe and T. Fuchigami, *Angew. Chem., Int. Ed.*, 2010, **49**, 10136; (f) Z. Gu and Y. Tang, *Lab Chip*, 2010, **10**, 1946.
- H. P. Zheng, I. Lee, M. F. Rubner and P. T. Hammond, *Adv. Mater.*, 2002, **14**, 569.
- (a) X. P. Jiang, H. P. Zheng, S. Gourdin and P. T. Hammond, *Langmuir*, 2002, **18**, 2607; (b) H. P. Zheng, M. F. Rubner and P. T. Hammond, *Langmuir*, 2002, **18**, 4505.
- H. H. Ko, C. Y. Jiang and V. V. Tsukruk, *Chem. Mater.*, 2005, **17**, 5489.
- (a) Y. X. Lu, X. L. Chen, W. Hu, N. Lu, J. Q. Sun and J. C. Shen, *Langmuir*, 2007, **23**, 3254; (b) C. He, Y. Long, J. Pan, K. Li, F. Liu, C. He, Y. Long, J. Pan, K. Li and F. Liu, *J. Mater. Chem.*, 2008, **18**, 2849.

- 
- 13 (a) H. Jang, S. Kim and K. Char, *Langmuir*, 2003, **19**, 3094; (b) J. Cho, H. Jang, B. Yeom, H. Kim, R. Kim, S. Kim, K. Char and F. Caruso, *Langmuir*, 2006, **22**, 1356.
- 14 (a) H. W. Shim, J. H. Lee, T. S. Hwang, Y. W. Rhee, Y. M. Bae, J. S. Choi, J. Han and C. S. Lee, *Biosens. Bioelectron.*, 2007, **22**, 3188; (b) B. Yuan, Y. Li, D. Wang, Y. Y. Xie, Y. Y. Liu, L. Cui, F. Q. Tu, H. Li, H. Ji, W. Zhang and X. Y. Jiang, *Adv. Funct. Mater.*, 2010, **20**, 3715.
- 15 (a) F. Hua, J. Shi, Y. Lvov and T. Cui, *Nano Lett.*, 2002, **2**, 1219; (b) F. Shi, Z. Q. Wang, N. Zhao and X. Zhang, *Langmuir*, 2005, **21**, 1599; (c) Y. P. Wang, P. Han, G. L. Wu, H. P. Xu, Z. Q. Wang and X. Zhang, *Langmuir*, 2010, **26**, 9736; (d) W. M. Moreau, *Semiconductor Lithography: Principles and Materials*; Plenum: New York, 1988.
- 16 P. P. Bontchev, S. Liu, J. L. Krumhansl and J. Voigt, *Chem. Mater.*, 2003, **15**, 3669.
- 17 (a) M. A. Reppy and B. A. Pindzola, *Chem. Commun.*, 2007, 4317; (b) A. C. S. Pires, N. F. F. Soares, L. H. M. da Silva, M. C. H. Silva, A. B. Mageste, R. F. Soares, A. V. N. C. Teixeira and N. J. Andrade, *J. Phys. Chem. B*, 2010, **114**, 13365.
- 18 M. D. Mowery, A. C. Smith and C. E. Evans, *Langmuir*, 2000, **16**, 5998.
- 19 D. J. Ahn and J. M. Kim, *Acc. Chem. Res.*, 2008, **41**, 805.
- 20 (a) B. Valeur, *Molecular Fluorescence: Principles and Applications*; Wiley-VCH Verlag, 2001; p 131; (b) J. R. Lakowicz, *Principles of Fluorescence Spectroscopy*; Springer Verlag, 2006; chapter 10.
- 21 (a) M. Schott, *J. Phys. Chem. B*, 2006, **110**, 15864; (b) O. J. Dautel, M. Robitzer, J. P. L. Porte, S. F. Spirau and J. J. E. Moreau, *J. Am. Chem. Soc.*, 2006, **128**, 16213.
- 22 H. J. Bowley, D. L. Gerrard and W. F. Maddams, *Makromol. Chem.*, 1987, **188**, 899.
- 23 S. Dei, A. Matsumoto and A. Matsumoto, *Macromolecules*, 2008, **41**, 2467.
- 24 P. P. Bontchev, S. Liu, J. L. Krumhansl and J. Voigt, *Chem. Mater.*, 2003, **15**, 3669.